Molecular Therapy
Original Article

Targeting the hepatitis B cccDNA with a sequence-specific ARCUS nuclease to eliminate hepatitis B virus *in vivo*

Cassandra L. Gorsuch,[1] Paige Nemec,[1] Mei Yu,[2] Simin Xu,[2] Dong Han,[2] Jeff Smith,[1] Janel Lape,[1] Nicholas van Buuren,[2] Ricardo Ramirez,[2] Robert C. Muench,[2] Meghan M. Holdorf,[2] Becket Feierbach,[2] Greg Falls,[1] Jason Holt,[1] Wendy Shoop,[1] Emma Sevigny,[1] Forrest Karriker,[1] Robert V. Brown,[1] Amod Joshi,[1] Tyler Goodwin,[1] Ying K. Tam,[3] Paulo J.C. Lin,[3] Sean C. Semple,[3] Neil Leatherbury,[1] William E. Delaney IV,[2] Derek Jantz,[1] and Amy Rhoden Smith[1]

[1]Precision BioSciences Inc, Durham, NC 27701, USA; [2]Gilead Sciences, Inc, Foster City, CA 94404, USA; [3]Acuitas Therapeutics, Vancouver, BC V6T 1Z3, Canada

Persistence of chronic hepatitis B (CHB) is attributed to maintenance of the intrahepatic pool of the viral covalently closed circular DNA (cccDNA), which serves as the transcriptional template for all viral gene products required for replication. Current nucleos(t)ide therapies for CHB prevent virus production and spread but have no direct impact on cccDNA or expression of viral genes. We describe a potential curative approach using a highly specific engineered ARCUS nuclease (ARCUS-POL) targeting the hepatitis B virus (HBV) genome. Transient ARCUS-POL expression in HBV-infected primary human hepatocytes produced substantial reductions in both cccDNA and hepatitis B surface antigen (HBsAg). To evaluate ARCUS-POL *in vivo*, we developed episomal adeno-associated virus (AAV) mouse and non-human primate (NHP) models containing a portion of the HBV genome serving as a surrogate for cccDNA. Clinically relevant delivery was achieved through systemic administration of lipid nanoparticles containing ARCUS-POL mRNA. In both mouse and NHP, we observed a significant decrease in total AAV copy number and high on-target indel frequency. In the case of the mouse model, which supports HBsAg expression, circulating surface antigen was durably reduced by 96%. Together, these data support a gene-editing approach for elimination of cccDNA toward an HBV cure.

INTRODUCTION

Following hepatitis B virus (HBV) infection, 5%–10% of adults and up to 90% of young children fail to produce an immune response adequate to clear the infection and subsequently develop chronic hepatitis B (CHB).[1] Worldwide, approximately 240 million people have CHB, and these patients often progress to liver cirrhosis, hepatocellular carcinoma, and liver failure.[2,3] Long-term treatment with nucleos(t)ide analogues (NAs) provides durable on-treatment suppression of viral replication but is unable to directly target the covalently closed circular DNA (cccDNA) leading to life-long therapy. Furthermore, NAs are unable to completely suppress viral replication; therefore, low-level infectious virus persists for the majority of patients.[4]

HBV is a hepatotropic, partially double-stranded 3.2-kb DNA virus. On infection of human hepatocytes, the HBV genome enters the nucleus, undergoes a repair process, and is converted to cccDNA. Five overlapping mRNAs are produced from the HBV cccDNA, which results in the expression of HBV proteins necessary to complete the remainder of the viral life cycle.[5–8]

Hepatitis B surface antigen (HBsAg) is the major viral component of the envelope for infectious HBV particles. It is secreted in excess into patients' serum and thought to contribute to chronic immune dysfunction in patients.[9–11] In addition to cccDNA-derived HBsAg, HBsAg can also originate from integrated forms of HBV DNA.[12–14] The loss of HBsAg has been associated with improved patient outcomes, including reversal of cirrhosis, decreased risk of HCC, and prolonged survival. Sustained loss of HBsAg is considered an important clinical endpoint for HBV therapies and therefore a key parameter associated with functional cure.[15–18]

Genome editing has recently emerged as an attractive therapeutic approach, potentially offering a single-administration treatment with a lasting effect.[19–22] ARCUS endonucleases have demonstrated high levels of editing at various target sites in numerous models.[23–26] Additionally, ARCUS nucleases possess several attractive attributes for therapeutic application, including a single-component protein containing both a site-specific DNA recognition interface and

Received 20 December 2021; accepted 11 May 2022;
https://doi.org/10.1016/j.ymthe.2022.05.013.

Correspondence: Derek Jantz, Precision BioSciences Inc, E. Pettigrew Street, Durham, NC 27701, USA.
E-mail: derek.jantz@precisionbiosciences.com
Correspondence: Amy Rhoden Smith, Precision BioSciences Inc, E. Pettigrew Street, Durham, NC 27701, USA.
E-mail: amy.rhodensmith@precisionbiosciences.com

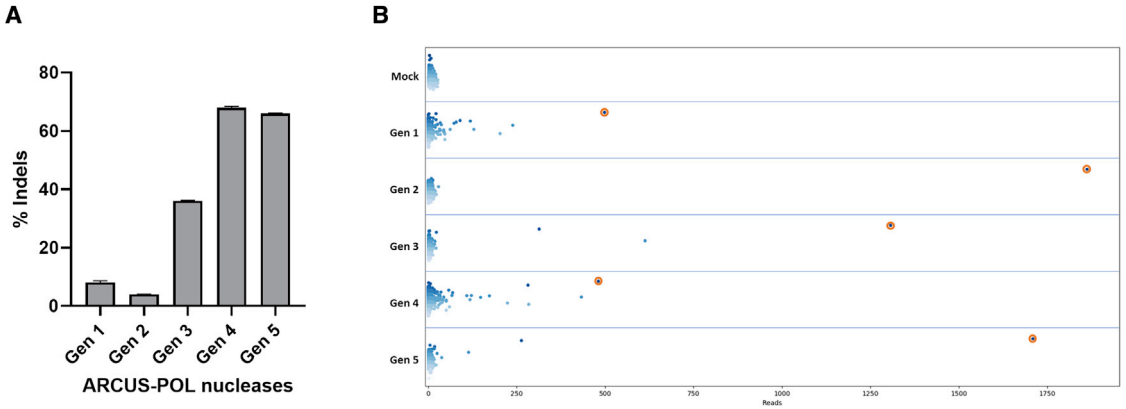

Figure 1. Optimization of nucleases targeting the HBV polymerase gene

(A) Nuclease activity as measured by indel frequency is shown for representative nucleases from each optimization cycle. On-target % indels quantified by droplet digital PCR (ddPCR) following nuclease treatment in Hep3B cells. (B) Semi-quantitative analysis of specificity measured by oligo-capture in HepG2-HBV cells following nuclease treatment. Individual genomic sites with incorporated probe are indicated as dots (blue represents off-target sites, orange represents the on-target site), with the darker blue dots representing sites with greater homology compared with the intended target site, and lighter-colored dots having more sequence variation. The read count indicates the number of times a site was recovered in the sequencing data, with higher read counts qualitatively correlating with higher frequency of editing.

endonuclease activity. The combination of the substrate-recognition and catalytic motifs into a single protein, encoded by ~1,100 bp, allows for both viral and non-viral delivery modalities and iterative improvements in both activity and specificity through protein engineering. In an effort toward achieving HBV cure, we engineered and optimized gene-editing ARCUS nucleases (ARCUS-POL) capable of specifically cleaving a 22-bp sequence in the HBV polymerase open reading frame (ORF). We hypothesized that a nuclease-mediated double-stranded break (DSB) would lead to degradation of cccDNA or generate mutated, replication-incompetent cccDNA, with both outcomes potentially reducing HBsAg and persistent viremia (Figure S1). Here, we demonstrate sustained reductions of extracellular HBsAg, reduction in cccDNA, and on-target editing in HBV-infected primary human hepatocytes (PHHs) following ARCUS-POL nuclease activity. Potential risks of utilizing a gene-editing approach to cut and degrade cccDNA include the possibility of integrating the cut viral DNA into the host genome and the introduction of chromosomal rearrangements. We show that nuclease specificity improvements result in decreased off-target editing, fewer nuclease-mediated viral DNA integrations, and elimination of chromosomal rearrangements.

HBV animal models supporting cccDNA formation are limited because of lack of susceptibility to HBV infection. Therefore, we have developed an episomal adeno-associated virus (AAV) mouse model and a novel non-human primate (NHP) model to assess the activity of the ARCUS-POL nuclease against a cccDNA surrogate *in vivo*. High levels of editing and degradation of the episomal AAV vector after lipid nanoparticle (LNP) delivery of the ARCUS-POL nuclease mRNA were observed in both models. Together these data demonstrate the viability of a gene-editing approach using the ARCUS-POL nuclease to decrease cccDNA and secreted HBsAg with the goal of achieving HBV cure.

RESULTS

Optimization of nucleases targeting the HBV polymerase gene

As previously reported,[26] ARCUS nucleases are engineered variants of the I-CreI homing endonuclease from *C. reinhardtii* that are designed to specifically recognize and cut a 22-bp sequence of choice. To assess a gene-editing strategy for HBV, nucleases were designed against a target site within the HBV polymerase ORF (nt 1,259–1,280) with high conservation across HBV genotypes and low predicted off-target editing activity in the human genome (Figure S2). Nucleases were initially characterized for on-target editing activity following electroporation of the mRNA in the human HCC-derived Hep3B cell line containing multiple integrated copies of HBV sequences. Specificity analysis was assessed using a semi-quantitative, unbiased oligo-capture assay. To simplify potential off-targeting readouts, this assay was performed in a HepG2 cell line generated to contain a single integration of a partial HBV genome (HepG2-HBV).

Five generations of ARCUS-POL nucleases (Gens 1–5) were created and optimized for activity and specificity through an iterative approach; representative nuclease data from each generation are shown in Figure 1. Initial rounds of optimization from Gen 1 nucleases yielded improvements in either on-target activity or on-target specificity. A final round of optimization aimed at specificity improvements yielded a Gen 5 nuclease with high levels of both on-target activity and specificity.

Specificity characterization of ARCUS-POL nucleases

To quantitate off-target editing frequencies of Gen 4 and Gen 5 ARCUS-POL nucleases in HBV-infected PHH cells, we designed PCR amplicons against sites, with the top three highest read counts recovered in the oligo-capture analysis, and indels were quantitated using next generation sequencing (NGS) (Table S1). At all off-target sites tested, the Gen 5 nuclease showed reduced off-target editing

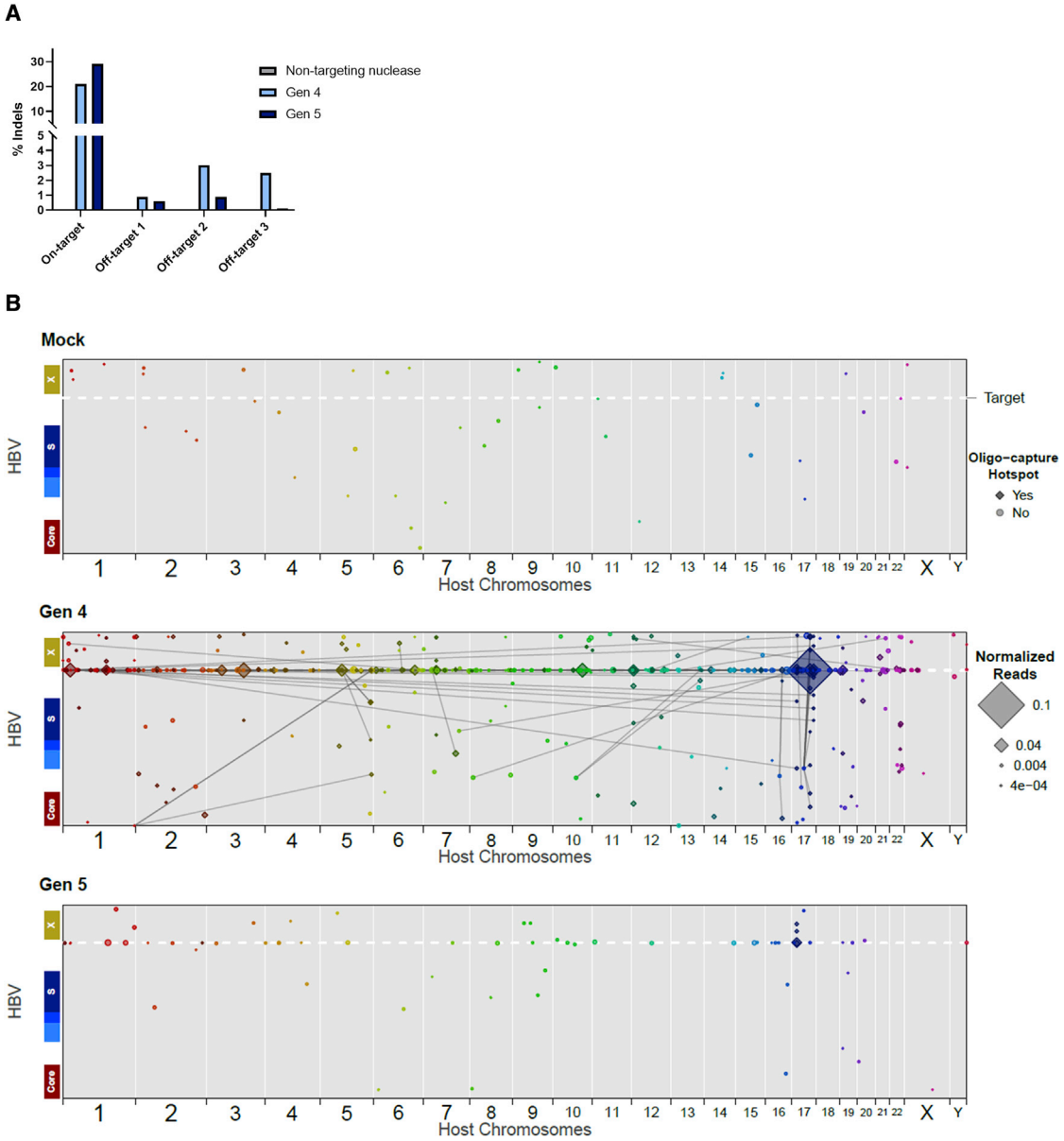

Figure 2. Specificity of Gen 4 and Gen 5 ARCUS-POL nucleases

(A) On-target indels in cccDNA and indels at three putative off-target sites identified in the oligo-capture assay were quantified by NGS. For on-target indels in cccDNA, total cellular DNA was treated with T5 exonuclease to enrich for cccDNA specifically prior to NGS. (B) Junctions between HBV and host DNA identified by targeted sequencing of PHHs mock treatment or treatment with Gen 4 or Gen 5 ARCUS nucleases. Junction points identified by oligo-capture analysis as potential off-target loci are shown as rhombi. Shape size reflects junction-site frequency after normalization with control host genes. Shape color indicates host chromosomes. Gray lines link junctions with at least 20 reads supporting a chromosomal translocation bridged by the integrated HBV. See also Figure S3.

compared with the Gen 4 nuclease with less than 1% indel formation for sites 1 and 2 and below the limit of detection (0.1% indels) for site 3 (Figure 2A). On-target indels in cccDNA were detected at 21% and 29% for the Gen 4 and Gen 5 ARCUS-POL nucleases, respectively (Figure 2A). Overall, these data indicate that the Gen 5 ARCUS-POL nuclease is both robust and specific for the intended target sequence.

A risk of utilizing a gene-editing approach for cutting and degrading cccDNA is the potential of the resulting linear viral DNA to integrate within DSBs in the host genome. To assess this risk, we utilized hybrid capture followed by long-read sequencing to identify viral DNA sequences with junctions to the host genomic sequence in HBV-infected PHH cells following mock transfection or transfection with Gen 4 or Gen 5 ARCUS-POL nucleases (Figures S3 and 2B).[27]

Integrations were observed at higher rates with the Gen 4 nuclease, with most insertions containing junctions between the host genome and the HBV genome at the ARCUS target site. Additionally, for the Gen 4 ARCUS-POL nuclease, we found that most integrations and translocations occurred at known off-target sites for this nuclease. Consistent with our specificity analysis, we observed fewer integrations of the HBV DNA and no detectable translocations in the host genomic DNA with the Gen 5 ARCUS-POL nuclease. Together, these data suggest that the high specificity of the Gen 5 ARCUS-POL nuclease results in fewer integrations of the HBV DNA into the host DNA and eliminated chromosomal rearrangements.

Antiviral activity of ARCUS-POL in HBV-infected PHHs

HBV-infected PHHs were used to assess the ability of the Gen 5 ARCUS-POL nuclease to specifically cut and degrade cccDNA and diminish HBsAg levels. Cells were transfected with Gen 5 ARCUS-POL nuclease mRNA or non-HBV-targeting nuclease mRNA on days 3 and 6 post-HBV infection. Supernatant and cellular DNA were collected at the time points indicated in Figure 3 and evaluated for cccDNA levels and editing, extracellular HBV DNA, and HBsAg levels. Human albumin levels were monitored to assess cell viability. Southern blot analysis revealed progressive declines in both relaxed circular HBV DNA (rcDNA) and cccDNA following Gen 5 ARCUS-POL nuclease mRNA transfection compared with non-targeting nuclease mRNA (Figure 3A). By day 17, Gen 5 ARCUS-POL nuclease treatment resulted in an ~85% reduction in cccDNA compared with cells receiving a non-targeting nuclease mRNA (Figure 3B).

In addition to the loss of cccDNA, it is possible for indels to occur at the nuclease target site (Figure S1). Using NGS, we found that the remaining cccDNA in cells treated with Gen 5 ARCUS-POL nuclease mRNA contained 29% indels by day 17 at the intended target site (Figure 3C). cccDNA editing and depletion resulted in an 80% reduction in extracellular HBV DNA and a 77% reduction in secreted HBsAg (Figures 3D and 3E). No significant difference was observed in secreted albumin with either the ARCUS-POL nuclease or the non-HBV-targeting nuclease, suggesting the reduction in HBsAg is specific to the HBV-targeting nuclease activity (Figure 3F). These data suggest that cutting by ARCUS-POL results predominantly in the degradation of cccDNA or, at a lower frequency, the introduction of indel mutations at the nuclease target site. Both outcomes likely contribute to the observed decreases in secreted viral DNA and HBsAg.

Activity of ARCUS-POL nuclease against integrated HBV DNA

Recent findings show integrated viral DNA within the host genome serves as a significant source of secreted HBsAg.[14] ARCUS-POL nuclease activity against integrated HBV was evaluated using an engineered HepG2 cell line (HepG2-sAg) containing a single integration of a partial HBV sequence that produces HBsAg. HepG2-sAg cells were electroporated with Gen 5 ARCUS-POL nuclease or mCherry mRNA, and indel formation and secreted HBsAg were evaluated. The average indels by day 9 post-transfection were 53% and 87% in cells receiving a 10 and 100 ng dose of mRNA, respectively (Figure 4A). In both doses, cells achieved maximal HBsAg reduction on day 6 post-transfection, with the 10 and 100 ng doses achieving 72% and 83% reduction of HBsAg, respectively (Figure 4B). These data demonstrate that the ARCUS-POL nuclease is also capable of reducing extracellular HBsAg from integrated HBV DNA.

ARCUS-POL nuclease activity in an episomal AAV mouse model

HBV tropism is limited to human hepatocytes, posing a challenge for testing therapeutic approaches *in vivo*. To evaluate the ARCUS-POL nuclease in mice, we developed an episomal AAV9 (AAV subtype 9) vector (AAV9-HBsAg) containing a partial HBV sequence driven by a liver-specific promoter to serve as a surrogate for cccDNA. On cutting of the episomal AAV, the AAV can either be degraded, repaired with an indel, or repaired back to wild-type, similar to cccDNA (Figure S1). NSG mice were administered AAV9-HBsAg vector intravenously (i.v.) and were then i.v. dosed with either an LNP containing the Gen 5 ARCUS-POL nuclease mRNA or phosphate-buffered saline (PBS) 3 weeks later. Serum HBsAg was monitored weekly, and liver AAV copies and indels assessed 4 weeks post-LNP administration.

Absolute AAV copy number was determined for both PBS- and nuclease-treated groups to assess degradation after nuclease cutting. Gen 5 ARCUS-POL nuclease significantly reduced AAV copy number compared with the PBS-treated group (Figure 5A). Additionally, the average indels detected in remaining AAVs was 86% in the nuclease-treated group (Figure 5B). Combined, the degradation and indel formation by the Gen 5 ARCUS-POL nuclease led to a 96% reduction of serum HBsAg level compared with PBS-treated animals starting 1 week after LNP administration and persisting until necropsy at week 7 (Figure 5C). Consistent with the reduction of serum HBsAg level, HBsAg immunohistochemical (IHC) staining on liver sections collected at necropsy also demonstrated a drastic reduction in HBsAg protein in Gen 5 ARCUS-POL-treated mice compared with PBS-treated mice (representative images in Figures 5D and S4). Together, these data demonstrate the ability of the Gen 5 ARCUS-POL nuclease to effectively cut episomal DNA leading to both degradation and indel formation at the target site. Although the ARCUS-POL site is located outside of the HBsAg ORF, the resulting indel formation and AAV degradation were able to dramatically reduce HBsAg *in vivo*.

ARCUS-POL nuclease activity in a novel episomal HBV NHP model

A significant challenge in HBV research is the lack of available NHP models susceptible to HBV infection.[28] To test the ARCUS-POL nuclease efficacy in cynomolgus macaques, we developed an AAV-HBsAg model similar to the mouse model described above. Because AAV8 has preferential liver tropism in NHPs, we changed the vector to AAV8-HBsAg.[29] The AAV8-HBsAg vector contains a partial HBV sequence that includes the ARCUS-POL target site and HBsAg ORF driven by a liver-specific promoter. For this study, an alternate Gen 5 ARCUS-POL nuclease (ARCUS-POL*) was selected because of increased on-target activity compared with the Gen 5 ARCUS-POL nuclease utilized in the other studies described (Figure S5).

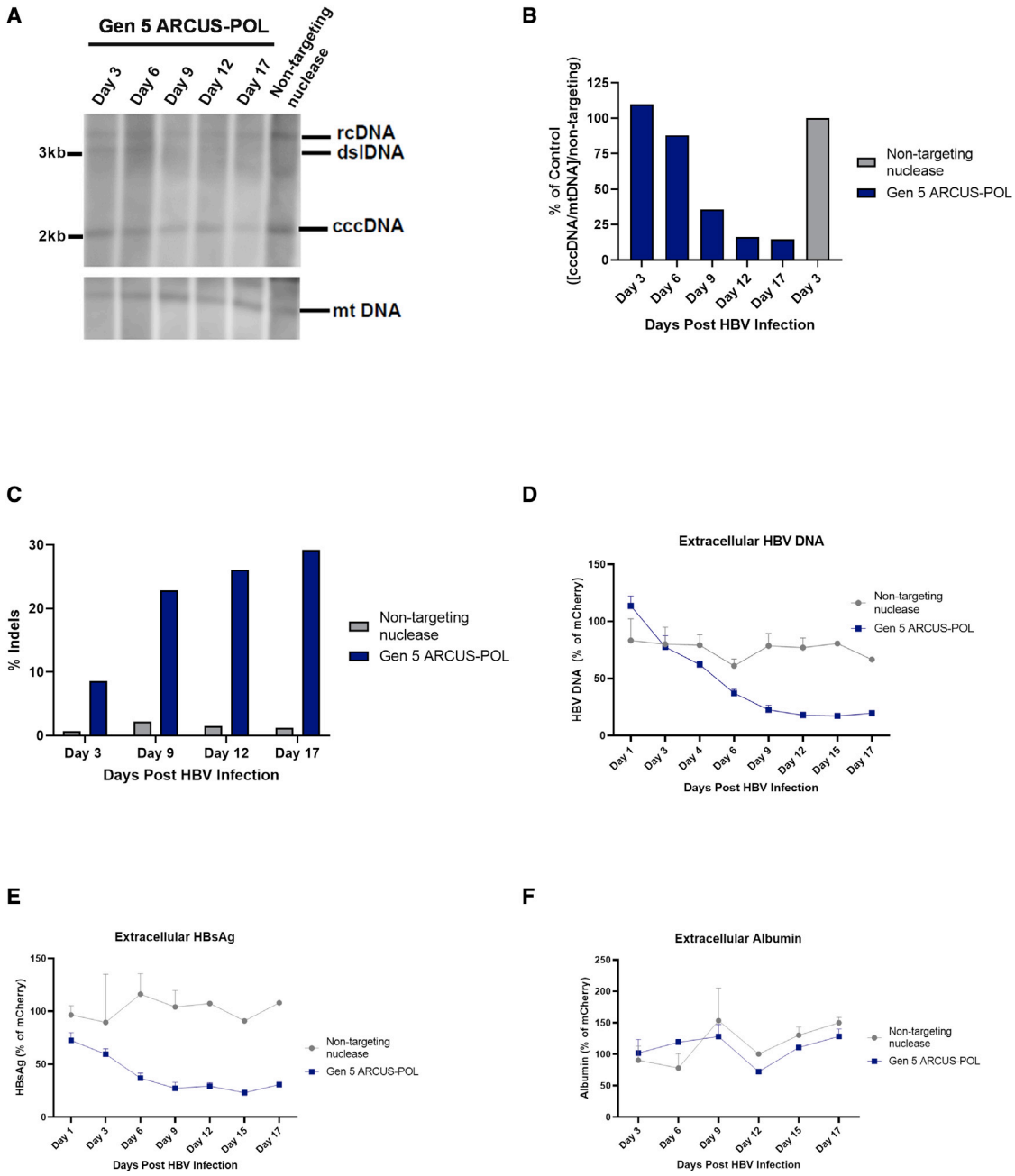

Figure 3. Antiviral effect of Gen 5 ARCUS-POL nuclease in HBV-infected PHHs

(A) Southern blot time-course analysis of HBV-infected PHHs following transfection of either Gen 5 ARCUS-POL or a non-HBV-targeting nuclease. (B) Densitometry was used to quantify cccDNA levels in PHH cells treated with Gen 5 ARCUS-POL or a non-targeting nuclease from the Southern blot. cccDNA levels were normalized to mtDNA and are shown as a percent of the normalized cccDNA levels of the non-targeting nuclease at day 3 post-HBV infection. (C) On-target indels in cccDNA were quantified by NGS. Prior to NGS, total cellular DNA was treated with T5 exonuclease to enrich for cccDNA. (D) Extracellular HBV DNA was quantified by a qPCR assay from PHH supernatant. (E) Extracellular HBsAg was quantified by CLIA from PHH supernatant. (F) Extracellular albumin was quantified by ELISA from PHH supernatant. Lines and error bars represent mean ± SD.

The groups included in the study and a study timeline are shown in Table 1 and Figure 6, respectively. Study groups included an LNP control group that received only ARCUS-POL* LNP, an AAV control group that received only the AAV8-HBsAg vector, and an experimental group that received both the AAV8-HBsAg vector and ARCUS-POL* LNP. The AAV8-HBsAg was i.v. administered on

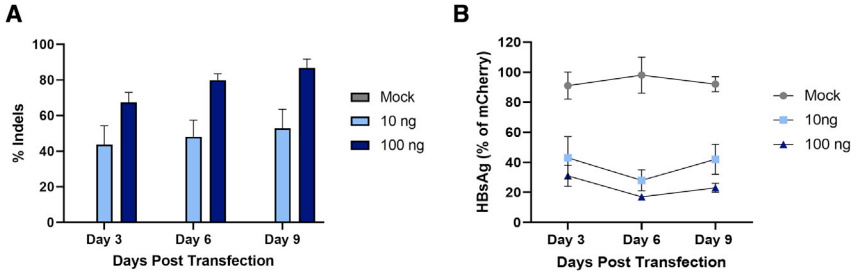

Figure 4. Targeting integrated viral DNA with Gen 5 ARCUS-POL nuclease

HepG2-sAg cells were electroporated with Gen 5 ARCUS-POL nuclease mRNA or control mCherry mRNA at concentrations of 10 and 100 ng or were mock transfected. On days 3, 6, and 9, cells were harvested for (A) on-target indel frequency analysis via ddPCR, and (B) supernatant was collected for extracellular HBsAg analysis via CLIA. Lines and error bars represent mean ± SD of biological replicates.

study day 8 to the AAV control and experimental groups, while the LNP control group was treated with PBS. On days 22 and 63, the LNP control and experimental groups were administered the ARCUS-POL* LNP, while the AAV control group was treated with PBS. Liver biopsies were performed for all groups on study days 36 and 77, and serum was collected throughout the study for HBsAg analysis.

Both AAV copy number and on-target indels in the AAV8-HBsAg vector were characterized from liver tissue collected during biopsies and at necropsy from the AAV control and experimental nuclease-treated groups (Figures 7A and 7C). No significant change in AAV copy number was observed between the nuclease-treated and AAV control groups following the first LNP administration; however, we did observe a significant reduction in AAV8-HBsAg abundance in the liver following the second LNP dose, which was maintained until necropsy (Figure 7A). This observation is consistent with other liver-targeted gene therapy approaches.[23,24] In addition to the molecular analysis of AAV copy number, *in situ* hybridization (ISH) using probes specific to the AAV8-HBsAg vector was conducted on liver sections obtained at each biopsy. We observed broad transduction of hepatocytes by AAV8-HBsAg and a qualitative reduction in AAV8-HBsAg present in the nuclease-treated animals compared with AAV control animals (Figure 7B). Furthermore, we observed increasing levels of on-target indel formation throughout the study. Animals receiving ARCUS-POL* LNP had an average of 9% indels at the first liver biopsy, 34% indels at the second liver biopsy, and 44% indels at necropsy (Figure 7C). Together these data demonstrate the ability of the ARCUS-POL* nuclease to cut episomal AAV8-HBsAg in NHPs, leading to reduced AAV genome copies and indels at the intended target site.

Serum samples were analyzed throughout the study for HBsAg and serum chemistry to monitor tolerability. Despite steroid immunosuppression, serum HBsAg decreased quickly over time and was below the limit of detection by day 36 for both the AAV control and nuclease-treated groups, suggesting immune clearance of the antigen. This prevented the assessment of nuclease activity on HBsAg production (Figure 5D). Transient elevations in alanine aminotransferase (ALT), aspartate transaminase (AST), lactate dehydrogenase (LDH), creatine kinase (CK), and several cytokines (e.g., from a multi-cytokine panel) were observed following LNP administration but returned to baseline within a week (Figures S6 and S7). Treatments were well tolerated in the animals, and the transient increases in serum chemistry biomarkers did not correlate with adverse microscopic findings in either the liver biopsy or terminal necropsy samples (data not shown). Although HBsAg was not an effective biomarker for efficacy in this NHP study, the episomal AAV model demonstrates efficient cutting, degradation, and on-target editing of ARCUS-POL using a cccDNA surrogate.

DISCUSSION

CHB is a major global health concern and one of the principal causes of chronic liver disease, cirrhosis, and hepatocellular carcinoma. A majority of CHB patients on long-term nucleos(t)ide therapy are unable to completely suppress viral replication; therefore, low-level infectious virus remains a contributor to the maintenance and persistence of infection.[4] Recent data have demonstrated that rate of transcriptionally active, and potentially mutagenic, viral integrations into the host genome is closely linked for HBV DNA levels.[30] As a result, the elimination of cccDNA is often cited as crucial to achieve HBV cure.[31]

In recent years, gene editing, particularly CRISPR-Cas9 and variants, has been explored as a potentially curative therapeutic approach for HBV but is hampered by CRISPR-Cas9 specificity, the potential for chromosomal translocations after a DSB, and delivery.[32] Here, we have developed an ARCUS nuclease with high on-target activity and specificity against the HBV polymerase gene with no detectable chromosomal translocations in a PHH infection model. Our studies show that ARCUS-POL can target cccDNA and integrated HBV DNA *in vitro*, resulting in robust HBsAg decline. Additionally, we have developed both mouse and NHP models to assess *in vivo* HBV gene editing with ARCUS using clinically translatable LNP/mRNA delivery. Our NHP model represents a novel way to assess gene editing for HBV in a large mammal, and this is, to our knowledge, the first report of gene editing in an HBV NHP model.

One surprising result was the reduction of HBsAg after editing downstream of the HBsAg ORF. However, given the overlapping transcript arrangement of the HBV genome, the nuclease target site falls within the 3′ untranslated region (UTR) of the HBsAg transcript, which is upstream of the polyadenylation sequence that is shared across all HBV transcripts. Previous studies have indicated this region may be important for transcript stability and/or export of mRNA out of the nucleus.[33–35] In fact, the region of the HBV genome where the

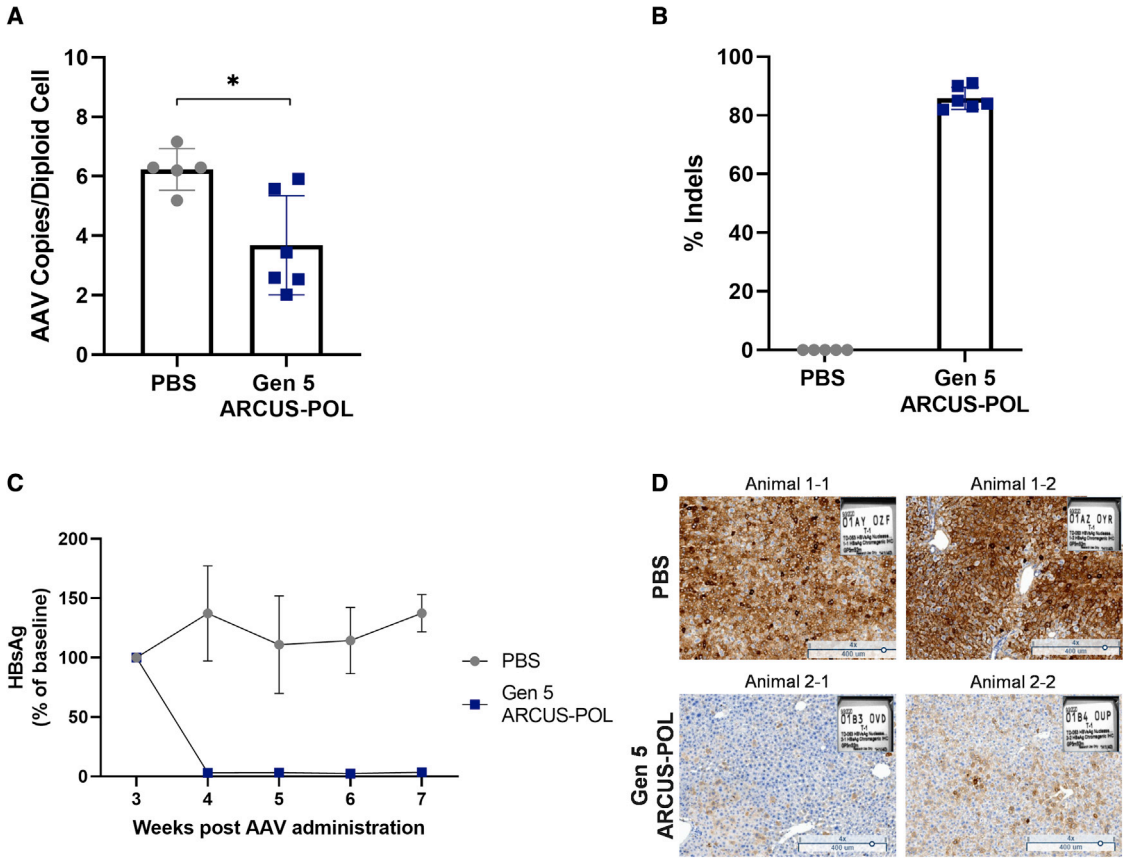

Figure 5. Gen 5 ARCUS-POL nuclease evaluation in an episomal AAV mouse model

Three weeks after AAV9-HBsAg administration, NSG mice were i.v. dosed with an LNP containing Gen 5 ARCUS-POL nuclease mRNA at 2 mg/kg. Blood draws were performed weekly, and animals were sacrificed 4 weeks post-LNP administration. At sacrifice, livers were harvested, and genomic DNA was extracted and assessed for (A) AAV copy number per diploid cell and (B) indel analysis at the target site present on the AAV9-HBsAg vector. (C) Serum was isolated from blood samples and analyzed for HBsAg via CLIA. (D) Immunohistochemistry for HBsAg detection was performed on liver tissue from necropsy (scale bars: 400 μm). Lines and error bars represent mean ± SD. Statistical analysis was performed using Mann-Whitney's two-tailed test. *$p \leq 0.05$. See also Figure S4.

ARCUS-POL site (bp 1,259–1,280) is located has been noted as hyperconserved across viral variants, suggesting a vital role for the virus.[36,37]

In addition to *in vitro* activity against cccDNA, we show *in vivo* efficacy using surrogate cccDNA models and LNP delivery of ARCUS-POL. We utilized an episomal AAV vector (AAV-HBsAg) containing a partial HBV DNA sequence that was introduced through systemic AAV administration to NSG mice or NHPs. *In vivo* efficacy using this cccDNA surrogate in NSG mice demonstrated a robust and sustained reduction (96%) of secreted HBsAg. Liver tissue collected at necropsy further showed reductions in AAV copy numbers and a high percentage of indel on-target editing at the ARCUS-POL site.

Despite utilizing immunosuppression throughout NHP studies, durable secretion of HBsAg was not maintained from the AAV vector, negating our ability to use HBsAg as a serum biomarker for editing. However, we were able to quantify molecular readouts of nuclease activity through editing of the AAV-HBsAg vector and vector copy number in serial liver biopsies. We demonstrate a 70% decrease in AAV-HBsAg genome copy number and 44% editing of the remaining AAV-HBsAg following two ARCUS-POL LNP administrations. Combining these two metrics, we estimate nuclease engagement with the AAV-HBsAg cccDNA surrogate resulting in either editing or degradation of 83% compared with control animals. Transient elevations of ALT, AST, and select cytokines were observed following LNP administration, but the ARCUS-POL nuclease was overall well tolerated. This represents a clinically translatable and efficacious delivery approach for targeting HBV DNA.

To address potential safety concerns relating to genomic integration of linearized viral DNA and the generation of translocation events, we examined viral integrations and translocations in HBV-infected PHH following ARCUS-POL nuclease treatment using HBV hybrid capture and long-read sequencing. Viral integrations and translocations were highly correlated to specificity of the ARCUS-POL

Table 1. Episomal HBV-AAV NHP study groups

Group	No. of animals	Dose level AAV (vector genomes (VG)/kg)	Dose level LNP (mg/kg)
LNP control (PBS + LNP)	2	0	2.0
AAV control (AAV + PBS)	4	6×10^{12}	0
Nuclease treated (AAV + LNP)	3[a]	6×10^{12}	2.0

[a]AAV8 nAb testing on serum obtained from NHPs on study day 8, prior to AAV8-HBsAg administration, revealed that one NHP of four in the nuclease-treated group had seroconverted against AAV8 and was therefore excluded from any data analysis.

nuclease, with the site of integrations and translocations located primarily at known off-target sites. Many of the viral integrations showed junctions between the host DNA and the viral DNA at the nuclease on-target site, suggesting the integrations were mediated by linearization of the viral DNA after nuclease cutting and may lead to chromosomal translocations. Specificity improvements in the Gen 5 ARCUS-POL nuclease greatly diminished the number of viral integrations and eliminated chromosomal translocations. Thus, nuclease specificity is paramount to minimize the frequency of integrations and eliminate chromosomal translocations between viral integrations. Although we still observe increased levels of viral integrations after editing with the Gen 5 ARCUS-POL nuclease compared with mock-transfected cells, we expect these integrations to be transcriptionally inactive given their genomic orientation and represent lower risk than integrations that would continue to accumulate over the natural life cycle of a chronic HBV infection.

Several promising therapeutic approaches for treating CHB have achieved significant reductions in HBsAg in clinical trials.[38] However, because these approaches do not eliminate cccDNA, viral reactivations may occur. The gene-editing approach described here aims to eliminate HBV cccDNA by using a transiently delivered, sequence-specific ARCUS nuclease and could offer a novel, curative therapy for patients.

MATERIALS AND METHODS

Cell culture and reagents

Hep3B and HepG2 cells were procured from ATCC and maintained in Eagle's minimal essential medium (EMEM; ATCC, Manassas, VA, USA) with 1% penicillin-streptomycin-glutamine (Thermo Fisher, Waltham, MA, USA) and 5% fetal bovine serum (FBS; Thermo Fisher) and grown in 5% CO_2, 37°C humidity-controlled incubators. Cryopreserved PHHs were purchased from BioreclamationIVT (Westbury, NY, USA). PHHs were seeded in Williams' Medium E (WME; Life Technologies, Carlsbad, CA, USA) in collagen-coated six-well plates (Corning; Corning, NY, USA).

Nuclease development and optimization

Precision BioSciences maintains a collection of proprietary I-CreI libraries that can be selected in directed evolution to recognize new target sequences. Directed evolution was used to generate two I-CreI monomers that recognized each half of the ARCUS-POL target sequence. The monomer sequences were combined using BsaI cloning to generate a fused single-peptide sequence library. The fused library of HBV 1 and HBV 2 monomers was selected in directed evolution for the ability to cut the intended ARCUS-POL target sequence. The nuclease library was also counterselected for the ability to discriminate against and not cut close off-target sequences. Resulting nucleases were tested for activity against the ARCUS-POL target and for discrimination against close off-target sequences. The best initial nuclease, Gen 1, was further evaluated for off-target cutting using our modified oligo-capture assay. Specific amino acids that did not provide sufficient discrimination against the incorrect nucleotide were rerandomized, and further directed evolution was conducted to produce Gen 2. The specificity analysis using oligo-capture was repeated on each subsequent generation to identify new off-targets for counterselection and new areas of the nuclease for refinement until a nuclease with sufficient activity and minimal off-targeting was generated in Gen 5. All plasmids used in nuclease generation were custom-made.

Oligo-capture assay

HepG2-HBV cells were co-electroporated with 1 μg oligo pool and 1 μg nuclease mRNA per 1×10^6 cells using the Neon Transfection System (Thermo Fisher). Cells were harvested on day 2 postelectroporation, and genomic DNA was isolated via the Macherey-Nagel NucleoSpin Blood QuickPure kit (Macherey-Nagel, Allentown, PA, USA).

Genomic DNA was sheared to ~550 bp using the M220 Focused-ultrasonicator (Covaris, Woburn, MA, USA). Cleaved ends were repaired and DNA adapters ligated using the NEBNext Ultra II Library Prep Kit for Illumina (New England Biolabs [NEB], Ipswich, MA, USA). Fragments were amplified using two nested sets of primers specific to the integrated oligo and the ligated adapter. Amplicons were purified from agarose gels using NucleoSpin Gel and PCR Clean-up columns (Machery-Nagel). Cleaned fragments were prepared for sequencing using the NEBNext Ultra II Library Prep Kit for Illumina Kit (NEB) per kit directions. Samples were sequenced using a 2×150-bp paired-end run on the NextSeq 550 (Illumina, San Diego, CA, USA).

A custom reference was created by concatenating the sequence of the lentivirus used to produce the HepG2-HBV cell line to the hg38 human genomic reference. Sequencing reads were aligned to this reference using bwa-mem (http://bio-bwa.sourceforge.net/bwa.shtml). Alignment files were then processed through a series of custom scripts. Amplification duplicated reads were removed based on position and unique molecular identifier (UMI) sequence, and junctions between inserted oligo sequence and genomic sequence within 500-bp windows were identified. The location of nuclease cleavage was determined based on distance from the oligo insertion and number of base pair mismatches to the intended nuclease target site.

Individual genomic sites with incorporated oligo are indicated as blue dots, with the darker colored dots representing sites with greater

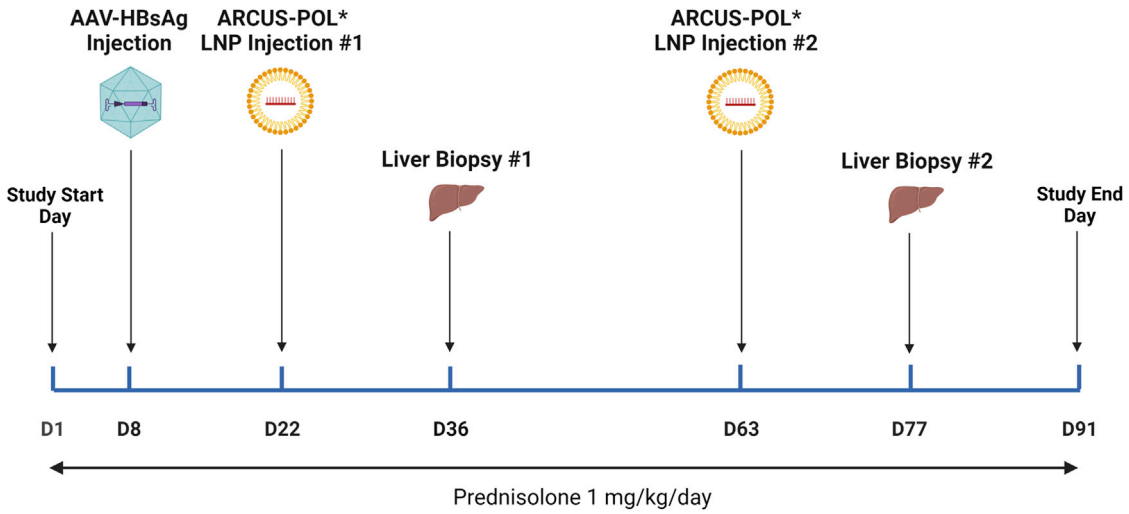

Figure 6. Episomal HBV-AAV NHP study timeline

All NHPs were given prednisolone at 1 mg/kg/day throughout the entire study. The AAV control and nuclease-treated groups were i.v. administered AAV8-HBsAg on day 8. At days 22 and 63, the LNP control and nuclease-treated groups were i.v. administered Gen 5 ARCUS-POL* LNP. Liver biopsies were taken for animals in all groups on days 36 and 77. Serum was collected throughout the study for HBsAg analysis, serum chemistry, and cytokine analysis. Schematic was created with BioRender.

homology compared with the intended target site, and lighter-colored dots having more sequence variation. The read count indicates the number of unique reads aligned at each site location with higher read counts indicating a higher likelihood of nuclease-mediated off-target editing. The on-target site is represented by a blue dot with an orange circle.

AAV plasmid and virus production

A partial HBV (genotype A) sequence was synthesized as a gBlock Gene Fragment (IDT, Coralville, IA, USA) and cloned into an AAV vector containing AAV2 ITR sequences and a liver-specific promoter. The plasmid was produced and purified by Aldevron (Fargo, ND, USA). Using this plasmid, recombinant AAV8 (rAAV8) and rAAV9 were produced and titered by SAB Technology (Philadelphia, PA, USA). Sequence of the AAV transgene was confirmed by PCR and Sanger sequencing of the virus preps.

mRNA production and LNP formulation

The ARCUS-POL nuclease sequences were cloned into a pRNA vector, which includes both 5′ and 3′ UTRs and a polyT repeat to serve as a template for a >100-bp poly(A) tail. The DNA template was linearized and purified using NucleoSpin Gel and PCR Clean-up columns (Machery-Nagel). *In vitro* mRNA transcription was performed using HiScribe T7 High Yield RNA synthesis kit (NEB), substituting with 2.5 mM N1-methyl-pseudouridine-modified NTP (TriLink BioTechnologies, San Diego, CA, USA) and 5 mM CleanCap AG (TriLink). DNase treatment was performed according to the manufacturer's protocol, and RNA was purified using the Promega SV total RNA isolation system. RNA concentration was determined by UV absorption using a NanoDrop (Thermo Fisher), and RNA quality was assessed on a 5200 Fragment Analyzer (Agilent Technologies, Santa Clara, CA, USA).

LNP production consisted of rapid mixing of an ethanolic solution of 1,2-distearoyl-sn-glycero-3-phosphocholine, cholesterol, a polyethylene glycol (PEG) lipid, and an ionizable cationic lipid with mRNA dissolved in an acidic acetate buffer using an in-line mixer. The PEG and ionizable lipids and LNP composition are described in patent applications WO 2015/199952 and WO 2017/075531A1. The post-in-line formulation was subjected to a Tangential Flow Filtration (Repligen, Waltham, WA, USA) to remove the ethanol and exchange to 1× PBS. The formulation was then filtered through a 0.2-μm filter and frozen down at −80°C in the presence of a cryoprotectant. The LNP had an average hydrodynamic diameter of <100 nm with a monodisperse distribution with a polydispersity index (PDI) <0.1 measured by dynamic light scattering (Malvern NanoZS Zetasizer, UK). The encapsulation efficiency was >90% when measured by the Ribogreen assay (Life Technologies).

HBV-infected PHH culture

PHH cells were infected with HBV genotype D at 500 viral genome equivalents in infection medium containing 4% PEG 8000 and 1.5% DMSO for 16 h at 37°C. Cells were washed with WME and cultured in maintenance medium containing 1.5% DMSO and 2% FBS. Nuclease transfections (2.5 μg mRNA per well in six-well plates) were conducted on 3 and 6 days post-HBV infection using the *Trans*IT-mRNA Transfection Kit (Mirus Bio, Madison, WI, USA) according to the manufacturer's instructions. Supernatant and cells were collected at indicated time points after HBV infection for various analyses.

Targeted PacBio and targeted Iso-Seq

Genomic DNA (gDNA) was sheared to ∼7.5 kbp using a G-tube (Covaris) and purified using the AMPure PB DNA beads (Pacific Biosciences, Menlo Park, CA, USA). Sheared DNA was barcoded using

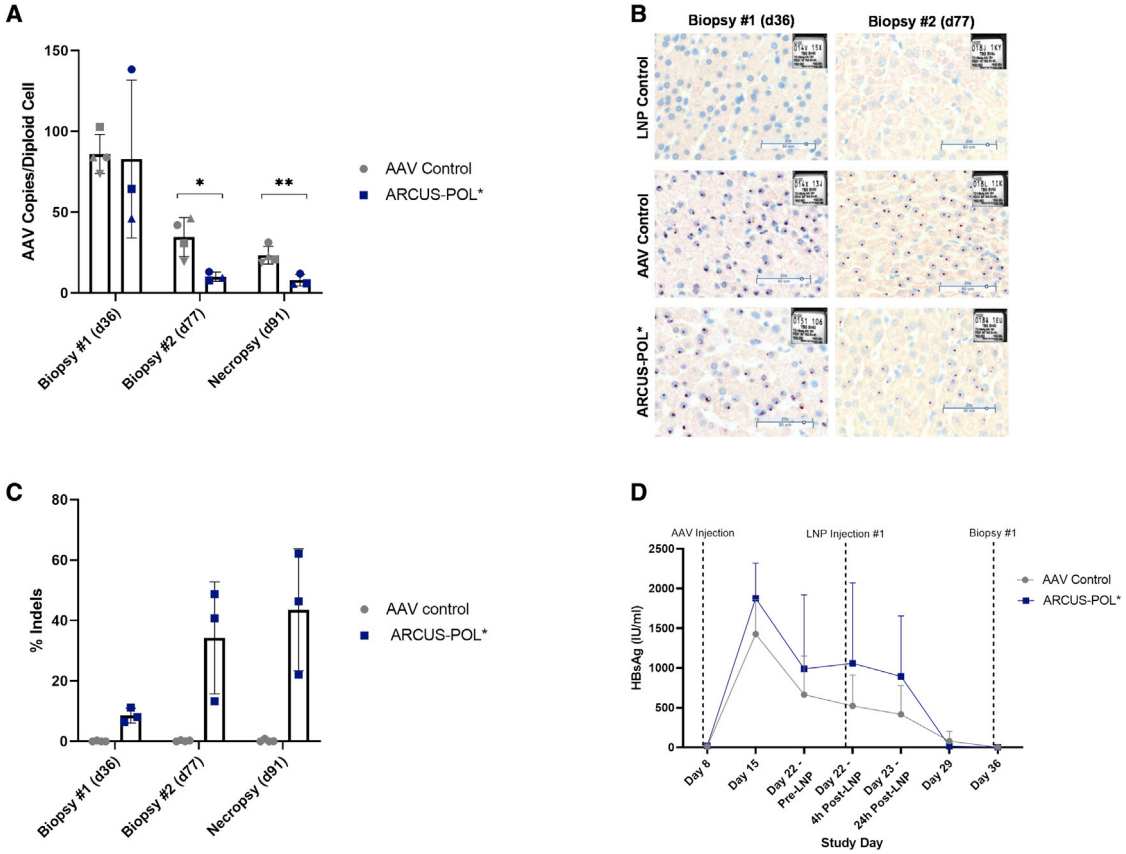

Figure 7. ARCUS-POL* nuclease evaluation in an episomal HBV-AAV NHP model

(A) AAV copy number was measured by ddPCR in liver tissue from biopsies and necropsy. (B) AAV was visualized by ISH in liver sections from biopsies (scale bars: 80 μm). (C) On-target indel analysis on the AAV8-HBsAg was measured via ddPCR. (D) Serum was analyzed for HBsAg levels. Lines and error bars represent mean ± SD. Statistical analysis was performed using two-tailed t test. *$p \leq 0.05$; **$p \leq 0.01$.

pre-annealed sample indexes (IDT) using the Kapa Hyper Prep library kit (Kapa Biosystems). Barcoded DNA was amplified using LA polymerase (Takara Bio, Shinga, Japan) and analyzed using a DNA high-sensitivity chip on the Bioanalyzer 2100 (Agilent). A custom panel of 120-bp biotinylated oligos was designed to be compatible with the xGen Lockdown platform (IDT). The panel consists of 144 HBV targeting probes and 16 probes targeting host genes. Barcoded DNA libraries were enriched for HBV sequences by incubating with our probe pool at 65°C for 4 h, capturing with streptavidin Dynabeads at 65°C for 45 min, and washing using the xGen Hybridization and Wash kit (IDT). Captured DNA sequences were amplified using the Takara LA polymerase. Enriched DNA libraries were sequenced on the Sequel II (Pacific Biosciences) at the Arizona Genomics Institute at the University of Arizona (Tucson, AZ, USA). Individual subreads were converted to circular consensus sequence (CCS) reads. CCS reads were used for analysis.

Extracellular HBV-DNA assay

PHH culture supernatants were treated with Turbo DNase (2 U/μL) (Thermo Fisher) according to the manufacturer's instructions before HBV DNA extraction using DNeasy 96 Blood & Tissue Kit (Qiagen, Germany). Total HBV DNA was quantified by qPCR using TaqMan Fast Advanced Master Mix (Applied Biosystems, Waltham, MA, USA), with the primer/probe set indicated in Table S2. DNA quantification was performed using the QuantStudio 7 Flex Real-Time qPCR system (Applied Biosystems).

Southern blot

PHH cells were lysed on days 3, 6, 9, 12, and 17 after HBV infection, and HBV DNA was extracted using Epicentre kits (Lucigen, Middleton, WI, USA) according to the manufacturer's instructions. A total of 30 μL DNA was separated by 1.2% agarose gel electrophoresis, followed by gel blotting, probe labeling, hybridization, and washing. Detection and quantification were performed using the ImageQuant LAS 4000 (General Electric, Schenectady, NY, USA). Probes were designed based on the HBV-AD38 sequence.

Albumin ELISA

Extracellular albumin from PHH supernatant was measured using a human albumin ELISA kit (RAB0603; Millipore Sigma, Burlington,

MA, USA) according to the manufacturer's instructions. In brief, PHH supernatant was collected at days 3, 6, 9, 12, 15, and 17; placed in a freezer set to maintain −80°C; and thawed for albumin ELISA analysis. The ELISA plate was read at an absorbance of 450 nm on a SpectraMax i3x microplate reader (Molecular Devices, San Jose, CA, USA), and albumin concentration values were calculated using a standard curve generated from purified albumin.

HepG2-sAg and HepG2-HBV cell line development

A lentiviral plasmid containing a partial HBV sequence and GFP sequence driven by a cytomegalovirus (CMV) promoter was transfected along with helper plasmids into Expi293 cells (Thermo Fisher) for lentivirus production. The resulting lentivirus was transduced into HepG2 cells (ATCC HB-8065) in the presence of 5 μg/mL polybrene. Transduction efficiency was determined by flow cytometry analyzing GFP^+ cells. Cells were sorted on the GFP bright population and ring cloned to isolate single cells, which were further characterized for GFP expression by flow cytometry, HBV sequence copy number, and the ability to produce HBsAg. The final clone chosen, HepG2-sAG, contains one HBV partial sequence, verified via Sanger sequencing, and produces HBsAg. The HepG2-HBV line was derived using the same conditions but with a slightly differing partial HBV sequence.

Episomal mouse model

All procedures for animal experimentation were approved by the Mispro Institutional Animal Care and Use Committee in accordance with their guidelines. NSG mice were purchased from The Jackson Laboratory (Bar Harbor, ME, USA). Female 8-week-old mice were maintained on a PicoLab Verified 75 IF irradiated diet according to the vendor's recommendations (LabDiet, St. Louis MO, USA). On study day 1, all mice received 5×10^{11} VG of the AAV9-HBsAg vector via retro-orbital (RO) injections. On study day 21, mice received either PBS or an LNP containing Gen 5 ARCUS-POL nuclease mRNA at 2 mg/kg via RO injections. Approximately 100 μL of blood was obtained from all animals by submandibular venipuncture at weekly intervals throughout the study. On study day 50, blood was collected, and the animals were perfused with PBS and euthanized. One piece of the median liver lobe was flash frozen on dry ice for gDNA extraction and molecular analyses. One sagittal section of the median liver lobe was harvested and transferred to 10% neutral-buffered formalin (NBF) for 24 h followed by paraffin embedding and sectioning at Experimental Pathology Labs (EPL; Morrisville, NC, USA). The primary antibody (BIORAD RbPol HBsAg) was diluted to 1:250, incubated on the tissue for 5 min, and then the polymer (anti-rabbit poly-horseradish peroxidase [HRP]-immunoglobulin G [IgG]) was incubated for 2 min. IHC staining was performed on BOND-RX using Leica's (Wetzlar, Germany) BOND Polymer Refine Detection kit. Images were scanned and acquired on the Leica Aperio VERSA (Wetzlar, Germany).

Indel and AAV genomic copies analyses

Genomic DNA was isolated from Hep3B cells, HepG2-sAg cells, mouse liver, or NHP liver using the Nucleospin Blood Quick Spin Kit (Macherey-Nagel) and from PHHs using Epicentre kits (Lucigen) according to the manufacturer's instructions. The genomic DNA was quantified by the DS-11 DeNovix Spectrophotometer/Fluorometer (DeNovix, Wilmington, DE, USA). For indel and copy number analysis, droplet digital PCR (ddPCR) was conducted using primers/probes indicated in Table S2. ddPCR amplifications were multiplexed in a 20-μL reaction containing 1× ddPCR Supermix for Probes (no dUTP; BioRad, Hercules, CA, USA), 250 nM of each probe, 900 nM of each primer, 5 U of HindIII-HF, and ∼50 ng cellular gDNA. Droplets were generated using a QX100 droplet generator (BioRad), and PCR was performed on a C1000 Touch thermal cycler (BioRad). Cycling conditions were as follows: 1 cycle of 95°C (2°C/s ramp) for 10 min, 45 cycles of 94°C (2°C/s ramp) for 10 s, 60°C (2°C/s ramp) for 30 s, 72°C (2°C/s ramp) for 1 min, 1 cycle of 98°C for 10 min, 4°C hold. Droplets were analyzed using a QX200 droplet reader (BioRad), and QuantaSoft analysis software (BioRad) was used to acquire and analyze data. Indel frequencies were calculated by dividing the number of positive droplets for the binding site probe by the number of positive droplets for the reference probe. AAV copies per diploid cell were calculated by dividing the number of positive droplets for the AAV copy number assay by the number of positive droplets of the single-copy genomic reference assay, and then multiplying by 2 to account for two genomes per diploid cell.

For off-target indels in PHH cells, total DNA was extracted, PCR amplicons were generated using primers indicated in Table S2, and Illumina NGS was conducted to quantify indels. To quantitate on-target indels in PHH cells, we extracted total DNA and treated T5 exonuclease (NEB) according to the manufacturer's protocol. Primers indicated in Table S2 were used to amplify across the nuclease target site, and Illumina NGS was utilized to quantitate indels.

For quantitation of indels using NGS at both on- and off-targets, amplicons were prepped for sequencing using the NEBNext Ultra II Library Prep Kit for Illumina Kit (NEB) per kit directions. Samples were sequenced using a 2 × 150-bp paired-end run on the NextSeq 550 (Illumina). Fastq files from reads 1 and 2 were stitched together using FLASH (https://ccb.jhu.edu/software/FLASH/) and aligned to a reference sequence using bwa-mem (http://bio-bwa.sourceforge.net/bwa.shtml). Custom scripts were developed to count insertions and deletions that overlap the intended target site (or putative off-target site) and to calculate percentage of indel-positive reads by dividing the number of reads containing mutations by the total number of reads per amplicon.

HBsAg analysis *in vitro* and *in vivo*

Circulating HBsAg levels in cell culture medium, mouse serum, and NHP serum were measured with an HBsAg-specific chemiluminescence assay (CLIA) (AutoBio, China), according to the manufacturer's instructions. Samples were analyzed using a SpectraMax i3x microplate reader (Molecular Devices) evaluating luminescence, and relative luminescence units (RLUs) were determined using a real-time calibration curve.

Episomal NHP model

Male cynomolgus macaques of Asian origin that were 2–5 years old were placed in a study. The NHP study was conducted at LabCorp

(previously Covance) (Madison, WI, USA) within a facility that is US Department of Agriculture registered, Association for Assessment and Accreditation of Laboratory Animal Care accredited, and Public Health Service assured. All procedures in this study were in compliance with the Animal Welfare Act, Guide for the Care and Use of Laboratory Animals, and Office of Laboratory Welfare.

NHP neutralizing AAV8 antibody screen

NHPs enrolled in the study were below the limit of detection (1:5 serum dilution) for AAV8 neutralizing antibodies (nAbs). An additional AAV8 nAb test was performed on serum from NHPs prior to AAV administration. The AAV8 vector used in the nAb assay contains the gene encoding β-galactosidase (β-gal) driven by a cytomegalovirus promoter (AAV8.CMV.LacZ.bGH; Lot# WL2575CS) and was made by the Vector Core Laboratory at the University of Pennsylvania (Philadelphia, PA, USA). The nAb titer values are reported as the reciprocal of the highest serum dilution that inhibits AAV8.CMV.LacZ.bGH transduction (β-gal expression) in HEK293 cells by $\geq$50%, compared with a naive mouse serum control. The limit of detection for the assay is 1:5 serum dilution. The variability of the assay is ± a single 2-fold serum dilution.

NHP study outline

All groups were treated with prednisolone (1 mg/kg) daily beginning on study day 1 through day 90 of the study period. The NHPs were divided into three groups. Group 1 was administered PBS on day 8 and ARCUS/LNP ARCUS-POL (2 mg/kg) on days 22 and 63. Group 2 was administered AAV8-7442 (6×10^{12} VG/kg) on day 8 and PBS on days 22 and 63. Group 3 was administered AAV8-7442 (6×10^{12} VG/kg) on day 8 and ARCUS/LNP ARCUS-POL* (2 mg/kg) on days 22 and 63. The AAV test article was diluted in PBS and administered via i.v. slow-bolus injection into a saphenous vein at a dose volume of 1 mL/kg over 2 min at a final dose of 6×10^{12} VG/kg. The ARCUS/LNP ARCUS-POL* test article was formulated in a sucrose buffer and dosed via i.v. infusion into a saphenous vein at a dose volume of 4 mL/kg over a 1-h period. All NHPs receiving LNP ARCUS-POL* were fasted overnight the day prior to dosing. On the day of LNP ARCUS-POL* dosing, animals were pre-treated with antihistamine (diphenhydramine; intramuscular [i.m.]: 2 mg/kg) 15–30 min prior to dose administration.

NHP blood and tissue collection

For hematology, clinical chemistry, and coagulation, whole blood (approximately 1 mL each) was collected via direct venipuncture of the femoral vein on study day 15 (predose phase), then once prior to dosing on study days 1, 8, 9 (clinical chemistry and hematology only), 15 (clinical chemistry and hematology only), 22, 24, 29, 36, 43, 50, 57, 63, 65, 70, 77, 84, and 91. Samples collected on study days 22 and 63 of the dosing phase were collected prior to LNP-ARCUS-POL* or vehicle control dosing and at approximately 4 and 24 h after LNP ARCUS-POL* or vehicle control administration.

For cytokine analysis, whole blood (approximately 1 mL) was collected via direct venipuncture of the femoral vein on study days 1 (predose and 4 and 24 h after dosing of prednisolone), 8 (predose and 24 h after AAV8 HBsAg or vehicle control administration), 22 and 63 (predose and 4 and 24 h after LNP ARCUS-POL* or vehicle control administration), 15, 29, 36, 70, and 77.

For HBsAg analysis, whole blood (approximately 1 mL each) was collected via direct venipuncture of the femoral vein on study days 1, 8, 15, 29, 36, 43, 50, 57, 70, 77, 84, and 91. Samples collected on study days 22 and 63 of the dosing phase were collected prior to LNP-ARCUS-POL* or vehicle control dosing and at approximately 4 and 24 h after LNP ARCUS-POL* or vehicle control administration.

Two 8-mm biopsy punches were taken from the left lateral lobe of the liver from all animals on study days 36 and 77 of the dosing phase. Animals were sedated with an i.m. injection of ketamine (5 mg/kg) and dexmedetomidine (0.02 mg/kg) prior to collection. Sedation was reversed with an i.m. injection of atipamezole (0.2 mg/kg). Animals were treated with a subcutaneous injection of meloxicam SR (0.6 mg/kg) following the biopsy procedure. The collection site was the abdominal cavity, and it was accessed using a laparoscopy procedure.

At study termination, all animals, having been fasted overnight, were anesthetized with sodium pentobarbital, exsanguinated, and necropsied. The liver (left lateral lobe, right lateral lobe, median lobe, and caudate lobe) was collected from all animals at the scheduled sacrifice. Two approximately 5-mm^3 sections were collected from each of the designated lobes for analysis.

NHP histopathology

All 10% NBF-preserved tissues were submitted for processing to slides. All processed tissues were examined microscopically with hematoxylin and eosin (H&E) staining by a board-certified veterinary pathologist at LabCorp (previously Covance) (Madison, WI, USA). NHP liver slides were stained using RNAscope 2.5 LSx Reagent Kit-RED and standard protocol established by Advanced Cell Diagnostics (ACD; Minneapolis, MN, USA) in conjunction with custom probes designed to detect the AAV.

SUPPLEMENTAL INFORMATION

Supplemental information can be found online at https://doi.org/10.1016/j.ymthe.2022.05.013.

ACKNOWLEDGMENTS

We thank Jeffrey Sunman, Armin Hekele, Clayton Beard, Dave Morris, Kristi Viles, and Paul Ray for their contributions to this work. This study was sponsored by Precision BioSciences Inc. and Gilead Sciences.

AUTHOR CONTRIBUTIONS

J.S. and D.J. designed and optimized the nucleases. C.L.G., P.N., J.S., J.L., W.S., E.S., A.J., N.B., R.R., D.H., B.F., R.C.M., S.X., and M.Y. designed and executed experiments and/or analyzed data. G.F., J.H.,

T.G., N.L., D.J., A.R.S., M.M.H., and W.E.D. contributed to experimental design and analysis of results. F.K. and R.V.B. developed and executed histochemical analyses of *in vivo* studies. Y.K.T., P.J.C.L., and S.C.S. designed and formulated the LNPs. C.L.G., P.N., A.R.S., R.C.M., and M.M.H. authored the manuscript.

DECLARATION OF INTERESTS

C.L.G., P.N., J.L., G.F., J.H., W.S., E.S., F.K., R.V.B., A.J., T.G., N.L., and A.R.S. received compensation as employees of Precision BioSciences Inc. J.S. and D.J. received compensation and equity as employees of Precision BioSciences Inc. M.Y., S.X., D.H., N.v.B., R.R., R.C.M., M.M.H., B.F., and W.E.D. received compensation as employees of Gilead Sciences. Y.K.T., P.J.C.L., and S.C.S. are employees of Acuitas Therapeutics.

REFERENCES

1. Zuckerman, A.J. (1996). Introduction. Windsor, Berkshire, United Kingdom, 25-26 July 1995. Gut *38*, S1–S70. https://doi.org/10.1136/gut.38.suppl_2.s1.
2. Trépo, C., Chan, H.L.Y., and Lok, A. (2014). Hepatitis B virus infection. Lancet *384*, 2053–2063. https://doi.org/10.1016/s0140-6736(14)60220-8.
3. Polaris Observatory Collaborators (2018). Global prevalence, treatment, and prevention of hepatitis B virus infection in 2016: a modelling study. The Lancet. Gastroenterol. Hepatol. *3*, 383–403.
4. Burdette, D.L., Lazerwith, S., Yang, J., Chan, H.L.Y., Delaney Iv, W.E., Fletcher, S.P., Cihlar, T., and Feierbach, B. (2022). Ongoing viral replication and production of infectious virus in patients with chronic hepatitis B virus suppressed below the limit of quantitation on long-term nucleos(t)ide therapy. PLoS One *17*, e0262516. https://doi.org/10.1371/journal.pone.0262516.
5. Urban, S., Schulze, A., Dandri, M., and Petersen, J. (2010). The replication cycle of hepatitis B virus. J. Hepatol. *52*, 282–284. https://doi.org/10.1016/j.jhep.2009.10.031.
6. Nassal, M. (2015). HBV cccDNA: viral persistence reservoir and key obstacle for a cure of chronic hepatitis B. Gut *64*, 1972–1984. https://doi.org/10.1136/gutjnl-2015-309809.
7. Tong, S., and Revill, P. (2016). Overview of hepatitis B viral replication and genetic variability. J. Hepatol. *64*, S4–S16. https://doi.org/10.1016/j.jhep.2016.01.027.
8. Schinazi, R.F., Ehteshami, M., Bassit, L., and Asselah, T. (2018). Towards HBV curative therapies. Liver Int. *38*, 102–114. https://doi.org/10.1111/liv.13656.
9. Burton, A.R., Pallett, L.J., McCoy, L.E., Suveizdyte, K., Amin, O.E., Swadling, L., Alberts, E., Davidson, B.R., Kennedy, P.T., Gill, U.S., et al. (2018). Circulating and intrahepatic antiviral B cells are defective in hepatitis B. J. Clin. Invest. *128*, 4588–4603. https://doi.org/10.1172/jci121960.
10. le Bert, N., Gill, U.S., Hong, M., Kunasegaran, K., Tan, D.Z.M., Ahmad, R., Cheng, Y., Dutertre, C.-A., Heinecke, A., Rivino, L., et al. (2020). Effects of hepatitis B surface antigen on virus-specific and global T cells in patients with chronic hepatitis B virus infection. Gastroenterology *159*, 652–664. https://doi.org/10.1053/j.gastro.2020.04.019.
11. Salimzadeh, L., le Bert, N., Dutertre, C.-A., Gill, U.S., Newell, E.W., Frey, C., Hung, M., Novikov, N., Fletcher, S., Kennedy, P.T., et al. (2018). PD-1 blockade partially recovers dysfunctional virus-specific B cells in chronic hepatitis B infection. J. Clin. Invest. *128*, 4573–4587. https://doi.org/10.1172/jci121957.
12. Tu, T., Budzinska, M.A., Shackel, N.A., and Urban, S. (2017). HBV DNA integration: molecular mechanisms and clinical implications. Viruses *9*, 75. https://doi.org/10.3390/v9040075.
13. Podlaha, O., Wu, G., Downie, B., Ramamurthy, R., Gaggar, A., Subramanian, M., Ye, Z., and Jiang, Z. (2019). Genomic modeling of hepatitis B virus integration frequency in the human genome. PLoS One *14*, e0220376. https://doi.org/10.1371/journal.pone.0220376.
14. Wooddell, C.I., Yuen, M.-F., Chan, H.L.-Y., Gish, R.G., Locarnini, S.A., Chavez, D., Ferrari, C., Given, B.D., Hamilton, J., Kanner, S.B., et al. (2017). RNAi-based treatment of chronically infected patients and chimpanzees reveals that integrated hepatitis B virus DNA is a source of HBsAg. Sci. Transl. Med. *9*, eaan0241. https://doi.org/10.1126/scitranslmed.aan0241.
15. Benias, P.C., and Min, A.D. (2011). Goals of antiviral therapy for hepatitis B: HBeAg seroconversion, HBsAg seroconversion, histologic improvement, and possible impact on risk of hepatocellular carcinoma. Curr. Hepat. Rep. *10*, 292–296. https://doi.org/10.1007/s11901-011-0112-4.
16. European Association For The Study Of The Liver (2012). EASL clinical practice guidelines: management of chronic hepatitis B virus infection. J. Hepatol. *57*, 167–185. https://doi.org/10.1016/j.jhep.2012.02.010.
17. Kim, G.-A., Lim, Y.-S., An, J., Lee, D., Shim, J.H., Kim, K.M., Lee, H.C., Chung, Y.-H., Lee, Y.S., and Suh, D.J. (2014). HBsAg seroclearance after nucleoside analogue therapy in patients with chronic hepatitis B: clinical outcomes and durability. Gut *63*, 1325–1332. https://doi.org/10.1136/gutjnl-2013-305517.
18. Zoulim, F., and Durantel, D. (2015). Antiviral therapies and prospects for a cure of chronic hepatitis B. Cold Spring Harb. Perspect. Med. *5*, a021501. https://doi.org/10.1101/cshperspect.a021501.
19. Yang, Y.-C., Chen, Y.-H., Kao, J.-H., Ching, C., Liu, I.-J., Wang, C.-C., Tsai, C.-H., Wu, F.-Y., Liu, C.-J., Chen, P.-J., et al. (2020). Permanent inactivation of HBV genomes by CRISPR/Cas9-Mediated non-cleavage base editing. Mol. Ther. Nucleic Acids *20*, 480–490. https://doi.org/10.1016/j.omtn.2020.03.005.
20. Stone, D., Long, K.R., Loprieno, M.A., de Silva Feelixge, H.S., Kenkel, E.J., Liley, R.M., Rapp, S., Roychoudhury, P., Nguyen, T., Stensland, L., et al. (2021). CRISPR-Cas9 gene editing of hepatitis B virus in chronically infected humanized mice. Methods Clin. Dev. *20*, 258–275. https://doi.org/10.1016/j.omtm.2020.11.014.
21. Yan, K., Feng, J., Liu, X., Wang, H., Li, Q., Li, J., Xu, T., Sajid, M., Ullah, H., Zhou, L., et al. (2021). Inhibition of hepatitis B virus by AAV8-derived CRISPR/SaCas9 expressed from liver-specific promoters. Front. Microbiol. *12*, 665184. https://doi.org/10.3389/fmicb.2021.665184.
22. Doudna, J.A. (2020). The promise and challenge of therapeutic genome editing. Nature *578*, 229–236. https://doi.org/10.1038/s41586-020-1978-5.
23. Wang, L., Breton, C., Warzecha, C.C., Bell, P., Yan, H., He, Z., White, J., Zhu, Y., Li, M., Buza, E.L., et al. (2021). Long-term stable reduction of low-density lipoprotein in nonhuman primates following in vivo genome editing of PCSK9. Mol. Ther. J. Am. Soc. Gene Ther. *29*, 2019–2029. https://doi.org/10.1016/j.ymthe.2021.02.020.
24. Wang, L., Smith, J., Breton, C., Clark, P., Zhang, J., Ying, L., Che, Y., Lape, J., Bell, P., Calcedo, R., et al. (2018). Meganuclease targeting of PCSK9 in macaque liver leads to stable reduction in serum cholesterol. Nat. Biotechnol. *36*, 717–725. https://doi.org/10.1038/nbt.4182.
25. Zekonyte, U., Bacman, S.R., Smith, J., Shoop, W., Pereira, C.V., Tomberlin, G., Stewart, J., Jantz, D., and Moraes, C.T. (2021). Mitochondrial targeted meganuclease as a platform to eliminate mutant mtDNA in vivo. Nat. Commun. *12*, 3210. https://doi.org/10.1038/s41467-021-23561-7.
26. MacLeod, D.T., Antony, J., Martin, A.J., Moser, R.J., Hekele, A., Wetzel, K.J., Brown, A.E., Triggiano, M.A., Hux, J.A., Pham, C.D., et al. (2017). Integration of a CD19 CAR into the TCR alpha chain locus streamlines production of allogeneic gene-edited CAR T cells. Mol. Ther. J. Am. Soc. Gene Ther. *25*, 949–961. https://doi.org/10.1016/j.ymthe.2017.02.005.
27. Ramirez, R., van Buuren, N., Gamelin, L., Soulette, C., May, L., Han, D., Yu, M., Choy, R., Cheng, G., Bhardwaj, N., et al. (2021). Targeted long-read sequencing reveals comprehensive architecture, burden, and transcriptional signatures from hepatitis B virus-associated integrations and translocations in hepatocellular carcinoma cell lines. J. Virol. *95*, e0029921. https://doi.org/10.1128/jvi.00299-21.
28. Guo, W.-N., Zhu, B., Ai, L., Yang, D.-L., and Wang, B.-J. (2018). Animal models for the study of hepatitis B virus infection. Zool. Res. *39*, 25–31. https://doi.org/10.24272/j.issn.2095-8137.2018.013.
29. Srivastava, A. (2016). In vivo tissue-tropism of adeno-associated viral vectors. Curr. Opin. Virol. *21*, 75–80. https://doi.org/10.1016/j.coviro.2016.08.003.
30. Hsu, Y.-C., Suri, V., Nguyen, M.H., Huang, Y.-T., Chen, C.-Y., Chang, I.-W., Tseng, C.-H., Wu, C.-Y., Lin, J.-T., Pan, D.Z., et al. (2022). Inhibition of viral replication reduces transcriptionally active distinct hepatitis B virus integrations with implications on host gene dysregulation. Gastroenterology *162*, 1160–1170.e1. https://doi.org/10.1053/j.gastro.2021.12.286.

31. Revill, P.A., Chisari, F.V., Block, J.M., Dandri, M., Gehring, A.J., Guo, H., Hu, J., Kramvis, A., Lampertico, P., Janssen, H.L.A., et al. (2019). A global scientific strategy to cure hepatitis B. Gastroenterol. Hepatol. *4*, 545–558. https://doi.org/10.1016/S2468-1253(19)30119-0.

32. Yang, Y.-C., and Yang, H.-C. (2021). Recent progress and future prospective in HBV cure by CRISPR/cas. Viruses *14*, 4.

33. Moolla, N., Kew, M., and Arbuthnot, P. (2002). Regulatory elements of hepatitis B virus transcription. J. Viral Hepat. *9*, 323–331. https://doi.org/10.1046/j.1365-2893.2002.00381.x.

34. Chen, A., Panjaworayan T-Thienprasert, N., and Brown, C.M. (2014). Prospects for inhibiting the post-transcriptional regulation of gene expression in hepatitis B virus. World J. Gastroenterol. *20*, 7993–8004. https://doi.org/10.3748/wjg.v20.i25.7993.

35. Zhou, T., Block, T., Liu, F., Kondratowicz, A.S., Sun, L., Rawat, S., Branson, J., Guo, F., Steuer, H.M., Liang, H., et al. (2018). HBsAg mRNA degradation induced by a dihydroquinolizinone compound depends on the HBV posttranscriptional regulatory element. Antiviral Res. *149*, 191–201. https://doi.org/10.1016/j.antiviral.2017.11.009.

36. Lim, C.S., and Brown, C.M. (2016). Hepatitis B virus nuclear export elements: RNA stem-loop α and β, key parts of the HBV post-transcriptional regulatory element. RNA Biol. *13*, 743–747. https://doi.org/10.1080/15476286.2016.1166330.

37. González, C., Tabernero, D., Cortese, M.F., Gregori, J., Casillas, R., Riveiro-Barciela, M., Godoy, C., Sopena, S., Rando, A., Yll, M., et al. (2018). Detection of hyper-conserved regions in hepatitis B virus X gene potentially useful for gene therapy. World J. Gastroenterol. *24*, 2095–2107. https://doi.org/10.3748/wjg.v24.i19.2095.

38. Soriano, V., Barreiro, P., Cachay, E., Kottilil, S., Fernandez-Montero, J.V., and de Mendoza, C. (2020). Advances in hepatitis B therapeutics. Ther. Adv. Infect. Dis. *7*. 204993612096502. https://doi.org/10.1177/2049936120965027.